1030 *Inorg. Chem.* **2011**, *50*, 1030–1038
DOI: 10.1021/ic101693v

Inorganic Chemistry
Article

Different *ortho* and *para* Electronic Effects on Hydrolysis and Cytotoxicity of Diamino Bis(Phenolato) "Salan" Ti(IV) Complexes

Dani Peri, Sigalit Meker, Cesar M. Manna, and Edit Y. Tshuva*

Institute of Chemistry, The Hebrew University of Jerusalem, 91904, Jerusalem, Israel

Received August 19, 2010

Bis(isopropoxo) Ti(IV) complexes of diamino bis(phenolato) "salan" ligands were prepared, their hydrolysis in 1:9 water/THF solutions was investigated, and their cytotoxicity toward colon HT-29 and ovarian OVCAR-1 cells was measured. In particular, electronic effects at positions *ortho* and *para* to the binding phenolato unit were analyzed. We found that *para* substituents of different electronic features, including Me, Cl, OMe, and NO_2, have very little influence on hydrolysis rate, and all *para*-substituted *ortho*-H complexes hydrolyze slowly to give O-bridged clusters with a $t_{1/2}$ of 1−2 h for isopropoxo release. Consequently, no clear cytotoxicity pattern is observed as well, where the largest influence of *para* substituents appears to be of a steric nature. These complexes exhibit IC_{50} values of 2−18 μM toward the cells analyzed, with activity which is mostly higher than those of Cp_2TiCl_2, $(bzac)_2Ti(OiPr)_2$ and cisplatin. On the contrary, major electronic effects are observed for substituents at the *ortho* position, with an influence that exceeds even that of steric hindrance. *Ortho*-chloro or -bromo substituted compounds possess extremely high hydrolytic stability where no major isopropoxo release as isopropanol occurs for days. In accordance, very high cytotoxicity toward colon and ovarian cells is observed for *ortho*-Cl and -Br complexes, with IC_{50} values of 1−8 μM, where the most cytotoxic complexes are the *ortho*-Cl-*para*-Me and *ortho*-Br-*para*-Me derivatives. In this series of *ortho*-substituted complexes, the halogen radius is of lesser influence both on hydrolysis and on cytotoxicity, while OMe substituents do not impose similar effect of hydrolytic stability and cytotoxicity enhancement. Therefore, hydrolytic stability and cytotoxic activity are clearly intertwined, and thus this family of readily available Ti(IV) salan complexes exhibiting both features in an enhanced manner is highly attractive for further exploration.

Introduction

The interest in metal based anticancer therapeutics is growing ever since the discovery of the antitumor properties of cisplatin.[1−3] High chelation affinity, attraction to electron rich molecules, variable coordination number and more, make it reasonable to assume that metals can mediate apoptosis through various pathways as can be evident from the cisplatin anticancer mechanism. However, finite types of tumors that can be treated with cisplatin and extreme toxic effects such as neurotoxicity, nephrotoxicity, and others that usually accompany this chemotherapeutic treatment encourage extensive study of other antitumor tactics, including the exploration of other metals. Other metal centers can lead to different antitumor pathways because of different coordination numbers, electronic characteristics, and so forth. Thus, the search for other transition metal based drugs revealed anticancer properties for much of the block d metal groups.[4−9] This includes Ti(IV) complexes with various cyclopentadienide or diketonato ligands, which demonstrate cytotoxic activity toward cisplatin-resistant and -sensitive cells with reduced side effects (Scheme 1).[10−19] However, rapid hydrolysis in aqueous environment because of the inherent oxophilic

*To whom correspondence should be addressed. Fax +97226584282. E-mail: tshuva@chem.ch.huji.ac.il.

(1) Barnes, K. R.; Lippard, S. J. *Met. Ions Biol. Syst.* **2004**, *42*, 143–177.
(2) Abu-Surrah, A. S.; Kettunen, M. *Curr. Med. Chem.* **2006**, *13*, 1337–1357.
(3) Cepeda, V.; Fuertes, M. A.; Castilla, J.; Alonso, C.; Quevedo, C.; Perez, J. M. *Anti-Cancer Agents Med. Chem.* **2007**, *7*, 3–18.
(4) Galanski, M.; Arion, V. B.; Jakupec, M. A.; Keppler, B. K. *Curr. Pharm. Des.* **2003**, *9*, 2078–2089.
(5) Desoize, B. *Anticancer Res.* **2004**, *24*, 1529–1544.
(6) Xu, G.; Cui, Y. B.; Cui, K.; Gou, S. H. *Prog. Chem.* **2006**, *18*, 107–113.
(7) Ott, I.; Gust, R. *Arch. Pharm. Chem. Life Sci.* **2007**, *340*, 117–126.
(8) Bruijnincx, P. C. A.; Sadler, P. J. *Curr. Opin. Chem. Biol.* **2008**, *12*, 197–206.
(9) Jakupec, M. A.; Galanski, M.; Arion, V. B.; Hartinger, C. G.; Keppler, B. K. *Dalton Trans.* **2008**, 183–194.
(10) Köpf-Maier, P.; Köpf, H. *Chem. Rev.* **1987**, *87*, 1137–1152.
(11) Köpf-Maier, P.; Köpf, H. *Struct. Bonding (Berlin)* **1988**, *70*, 103–185.
(12) Keppler, B. K.; Friesen, C.; Moritz, H. G.; Vongerichten, H.; Vogel, E. *Struct. Bonding (Berlin)* **1991**, *78*, 97–127.
(13) Christodoulou, C. V.; Eliopoulos, A. G.; Young, L. S.; Hodgkins, L.; Ferry, D. R.; Kerr, D. J. *Br. J. Cancer* **1998**, *77*, 2088–2097.
(14) Caruso, F.; Rossi, M.; Pettinari, C. *Expert Opin. Ther. Pat.* **2001**, *11*, 969–979.
(15) Meléndez, E. *Crit. Rev. Oncol. Hematol.* **2002**, *42*, 309–315.
(16) Caruso, F.; Rossi, M. *Mini-Rev. Med. Chem.* **2004**, *4*, 49–60.
(17) Kelter, G.; Sweeney, N. J.; Strohfeldt, K.; Fiebig, H.-H.; Tacke, M. *Anti-Cancer Drugs* **2005**, *16*, 1091–1098.
(18) Abeysinghe, P. M.; Harding, M. M. *Dalton Trans.* **2007**, 3474–3482.
(19) Strohfeldt, K.; Tacke, M. *Chem. Soc. Rev.* **2008**, *37*, 1174–1187.

Published on Web 01/07/2011

Scheme 1. Titanocene Dichloride (a) and Budotitane (b)

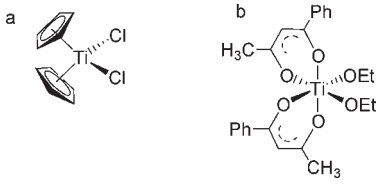

nature of Ti(IV) ions combined with electron poor configuration is the Achilles' heel of these compounds, which in turn led to failure in clinical trials.[12,13,20−23] In the presence of water, the labile groups (Cl, OEt) of titanocene dichloride (Cp_2TiCl_2, Scheme 1, a) and budotitane ($(bzac)_2Ti(OEt)_2$, Scheme 1, b) are hydrolyzed within minutes, followed by the more inert ligands (Cp, diketonato) within hours, leading to unidentified aggregates which hamper further mechanistic investigations. However, extensive studies of these compounds show tunable features of the anticancer properties.[24] Thus, a great challenge remains in the design and synthesis of better-suited Ti(IV) complexes that would demonstrate enhanced hydrolytic stability and improved antitumor properties.

Salans are well-known diamine bis(phenolato) compounds which have been used as chelating ligands for a wide variety of transition metals for various applications. We recently introduced the Ti(IV) salan complexes as a new family of highly cytotoxic compounds,[24−27] with cytotoxicity greater than that of Cp_2TiCl_2, $(bzac)_2Ti(OiPr)_2$, and cisplatin toward colon and ovarian cells. We have demonstrated that their particularly slow hydrolysis enables detailed studies in water-enriched environments, as the labile isopropoxo ligands hydrolyze within hours in 1:9 water/THF solutions, and the resulting salan-bound cluster does not further hydrolyze for days. We have detected a strong correlation between hydrolysis pathway and cytotoxicity, where formation of polynuclear O-bridged hydrolysis products were obtained for all cytotoxic complexes, and inactive complexes mostly released the free bis(phenol) ligand. Moreover, we have established that strong ligand binding enables its interaction with the cellular target as was particularly evident by a stereochemical study.[28] Furthermore, study of different derivatives of different steric and electronic properties by us,[24−27] followed by others,[29] have demonstrated that large steric bulk is of negative influence on cytotoxic activity, both when located near the metal center and when located on a peripheral area of the complex. This supports the notion that planarity is of importance for DNA intercalation; if indeed DNA is the cellular target.[12,28]

In the current study we investigated the effect of various electron donating and withdrawing groups on hydrolysis and cytotoxicity while comparing the *ortho* and *para* effects, with the assumption that increasing the electron donation ability of the ligand should provide favored complex features (Chart 1). Surprising patterns of influence both on hydrolysis and on cytotoxicity were observed.

Results and Discussion

In the current study we attempted to isolate electronic effects as much as possible and study their influence on the complex activity in particular at the *ortho* and at the *para* positions, with the notion that increasing the electron donation ability of the ligand should strengthen its metal binding and thus increase the complex hydrolytic stability, and consequently, its cytotoxicity. Synthesis of most ligand precursors $L^{1,2,4-8}H_2$ is achieved via a single step procedure according to known procedures,[30] from the commercially available diamine, substituted phenol, and formaldehyde. $L^3Ti(OiPr)_2$ is synthesized differently because of the electron withdrawal nature of the substituent, by a nucleophilic substitution on 2-chloromethyl-4-nitrophenol according to a published procedure.[31] Synthesis of Ti(IV) complexes was performed in analogy to known compounds under an inert atmosphere by mixing the ligand $L^{1-8}H_2$ with 1 equiv of $Ti(OiPr)_4$ in tetrahydrofuran (THF) at room temperature (RT) and stirring for about 2 h.[32−34] Removing the solvent under reduced pressure produced the product in quantitative yield, which may then be further recrystallized from diethylether to give yellow crystals or a yellow crystalline powder (Scheme 2).

Complexes $L^{1-8}Ti(OiPr)_2$ (Chart 1) all share similar structural features to known complexes of this type,[25,32,33,35,36] as evident mainly by NMR featuring the two AX systems of the methylene protons. They thus exhibit symmetry of C_2 because of *trans* binding of the phenolato donors and a *cis* configuration of the isopropoxo groups. A representative complex $L^5Ti(OiPr)_2$ was also analyzed by single crystal X-ray crystallography (Figure 1). A list of selected bond lengths and angles for this complex is given in Table 1. When comparing the structure of $L^5Ti(OiPr)_2$ to that of its analogues with only alkyl substituents on the aromatic rings, namely, with methyl groups *meta* and *para* to the phenolato oxygen atoms,[26] it is evident that the chloro substituents do not have a major effect on the coordination sphere of the Ti(IV) ion. For instance, the Ti−O1 and Ti−O2 distances vary between 1.91 and 1.93 Å, relative to a parallel value of 1.90 Å in the alkylated complex, and the O1−Ti−O2 angle of 163.0° is only slightly smaller than the 167.1° angle observed in the alkylated analogue.

(20) Toney, J. H.; Marks, T. J. *J. Am. Chem. Soc.* **1985**, *107*, 947–953.
(21) Schilling, T.; Keppler, K. B.; Heim, M. E.; Niebch, G.; Dietzfelbinger, H.; Rastetter, J.; Hanauske, A. R. *Invest. New Drugs* **1995**, *13*, 327–332.
(22) Korfel, A.; Scheulen, M. E.; Schmoll, H. J.; Grundel, O.; Harstrick, A.; Knoche, M.; Fels, L. M.; Skorzec, M.; Bach, F.; Baumgart, J.; Sass, G.; Seeber, S.; Thiel, E.; Berdel, W. E. *Clin. Cancer Res.* **1998**, *4*, 2701–2708.
(23) Caruso, F.; Massa, L.; Gindulyte, A.; Pettinari, C.; Marchetti, F.; Pettinari, R.; Ricciutelli, M.; Costamagna, J.; Canales, J. C.; Tanski, J.; Rossi, M. *Eur. J. Inorg. Chem.* **2003**, 3221–3232.
(24) Tshuva, E. Y.; Ashenhurst, J. A. *Eur. J. Inorg. Chem.* **2009**, 2203–2218.
(25) Shavit, M.; Peri, D.; Manna, C. M.; Alexander, J. S.; Tshuva, E. Y. *J. Am. Chem. Soc.* **2007**, *129*, 12098–12099.
(26) Peri, D.; Meker, S.; Shavit, M.; Tshuva, E. Y. *Chem.—Eur. J.* **2009**, *15*, 2403–2415.
(27) Tshuva, E. Y.; Peri, D. *Coord. Chem. Rev.* **2009**, *253*, 2098–2115.
(28) Manna, C. M.; Tshuva, E. Y. *Dalton Trans.* **2010**, *39*, 1182–1184.
(29) Immel, T. A.; Groth, U.; Huhn, T. *Chem.—Eur. J.* **2010**, *16*, 2775–2789.
(30) Tshuva, E. Y.; Gendeziuk, N.; Kol, M. *Tetrahedron Lett.* **2001**, *42*, 6405–6407.
(31) Whiteoak, C. J.; Britovsek, G. J. P.; Gibson, V. C.; White, A. J. P. *Dalton Trans.* **2009**, 2337–2344.
(32) Balsells, J.; Carroll, P. J.; Walsh, P. J. *Inorg. Chem.* **2001**, *40*, 5568–5574.
(33) Chmura, A. J.; Davidson, M. G.; Jones, M. D.; Lunn, M. D.; Mahon, M. F.; Johnson, A. F.; Khunkamchoo, P.; Roberts, S. L.; Wong, S. S. F. *Macromolecules* **2006**, *39*, 7250–7257.
(34) Gendler, S.; Segal, S.; Goldberg, I.; Goldschmidt, Z.; Kol, M. *Inorg. Chem.* **2006**, *45*, 4783–4790.
(35) Groysman, S.; Sergeeva, E.; Goldberg, I.; Kol, M. *Eur. J. Inorg. Chem.* **2005**, *2005*, 2480–2485.
(36) Yeori, A.; Groysman, S.; Goldberg, I.; Kol, M. *Inorg. Chem.* **2005**, *44*, 4466–4468.

Chart 1. Salan Complexes Studied

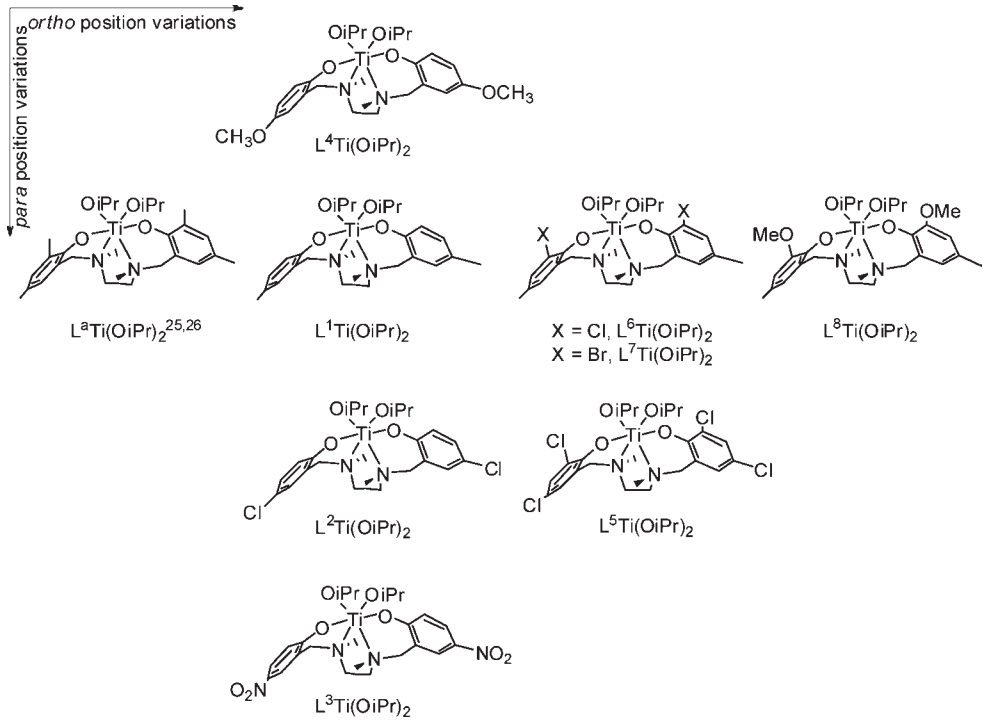

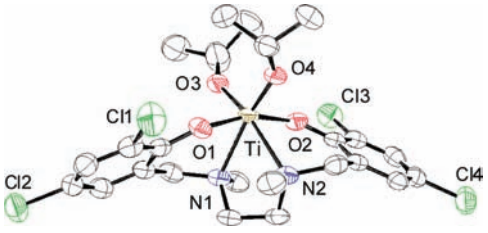

Figure 1. ORTEP drawing of $L^5Ti(OiPr)_2$ in 50% probability ellipsoids. H atoms were omitted for clarity.

Scheme 2. Synthesis of Diamino Bis(phenolato) Salan Complexes

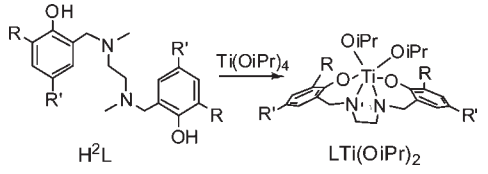

Hydrolysis Studies. As analogous complexes are generally stable for at least several hours in water enriched environments,[26] we were interested to establish the relative water resistance of this series of complexes as well. Therefore, we employed the NMR technique to monitor the hydrolysis reaction that occurs following D_2O addition to a d_8-THF solution of the $L^{1-8}Ti(OiPr)_2$ (Chart 1) to give a 1:9 D_2O/d_8-THF solution. The spectrum was measured every 5−10 min for up to 60 h, and the integration of selected signals was measured to gain insight on the complexes' decomposition process. In particular, the half-life of the isopropoxo ligands hydrolysis was measured by monitoring the integration of the septet signal of the CH group and/or the doublet of the methyl groups of the bound isopropoxo ligands. Other signals representing bound phenolato ligands in the original complex [Ti-ONNO], free bis(phenol) [HONNOH], and a new product of hydrolysis, were analyzed over time to provide information on the hydrolysis pathway, including reaction products and hydrolysis rates. A representative plot for $L^1Ti(OiPr)_2$ is shown in Figure 2, and a summary of $t_{1/2}$ values of hydrolysis of the isopropoxo groups for $L^{1-8}Ti(OiPr)_2$ is provided in Table 2, as calculated from the plots of isopropoxo release presented in Figure 3.

In an attempt to exclude steric effects as much as possible, in the series of $L^{1-4}Ti(OiPr)_2$ (Chart 1) the complexes were substituted only at the *para* position with substituents of markedly different electronic features. It is noteworthy that the steric effects at this position were also found in our previous studies to affect cytotoxicity.[26] The half-life values of isopropoxo hydrolysis for complexes $L^{1-4}Ti(OiPr)_2$ is in the same order of magnitude and varied between 1 and 2 h (Table 2, Figure 2,3), which corresponds to stability that generally exceeds that of titanocene dichloride and

Table 1. Selected Bond Lengths (Å) and Angles (deg) for $L^5Ti(OiPr)_2$

atoms	value	atoms	value
	Lengths		
O(1)−Ti	1.911(3)	N(1)−Ti	2.337(3)
O(2)−Ti	1.932(3)	N(2)−Ti	2.345(3)
O(3)−Ti	1.791(3)		
O(4)−Ti	1.806(3)		
	Angles		
O(4)−Ti−O(3)	106.08(13)	O(4)−Ti−N(1)	164.68(12)
O(4)−Ti−O(1)	92.73(12)	O(3)−Ti−N(1)	88.43(12)
O(3)−Ti−O(1)	97.67(13)	O(1)−Ti−N(1)	80.19(11)
O(4)−Ti−O(2)	96.62(12)	O(2)−Ti−N(1)	87.26(11)
O(3)−Ti−O(2)	93.29(12)	O(4)−Ti−N(2)	89.85(12)
O(1)−Ti−O(2)	163.05(11)	O(3)−Ti−N(2)	163.65(12)
N(1)−Ti−N(2)	76.08(11)	O(1)−Ti−N(2)	85.01(12)
		O(2)−Ti−N(2)	80.93(11)

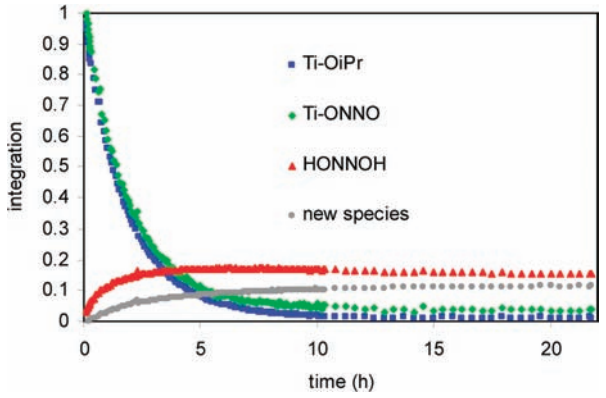

Figure 2. Representative plot of the integration of selected signals in the ^{1}H NMR spectrum of $L^1Ti(OiPr)_2$ versus time following addition of D_2O to a d_8THF solution of the complex at RT. All signals except for the "new species" were calibrated to represent a single proton. It is concluded that the new species is of reduced symmetry, and the selected signal represents reduced number of protons (vide infra).

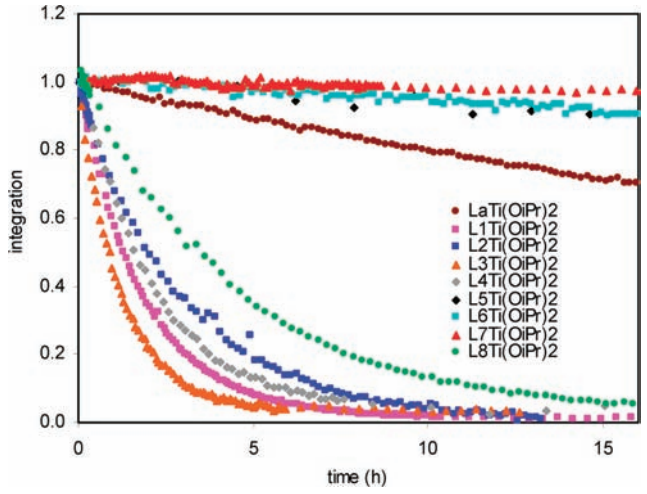

Figure 3. Plots of the integration of the Ti-OiPr signal in the ^{1}H NMR spectra of the complexes studied versus time following addition of D_2O to a d_8-THF solution of the complex at RT.

Table 2. $t_{1/2}$ (h) Values of Isopropoxo Release of $L^{1\text{-}8}Ti(OiPr)_2$ at 1:9 D_2O/d_8-THF Solution at RT

complex	substituents	$t_{1/2}$
$L^1Ti(OiPr)_2$	*o*-H-*p*-Me	2.1 ± 0.8
$L^2Ti(OiPr)_2$	*o*-H-*p*-Cl	2.1 ± 0.6
$L^3Ti(OiPr)_2$	*o*-H-*p*-NO_2	1.3 ± 0.7
$L^4Ti(OiPr)_2$	*o*-H-*p*-OMe	2.0 ± 0.2
$L^5Ti(OiPr)_2$	*o*-Cl-*p*-Cl	110 ± 10^a
$L^6Ti(OiPr)_2$	*o*-Cl-*p*-Me	130 ± 30^a
$L^7Ti(OiPr)_2$	*o*-Br-*p*-Me	290 ± 30^a
$L^8Ti(OiPr)_2$	*o*-OMe-*p*-Me	2.9 ± 0.4

[a] Estimated based on extrapolation.

budotitane.[12,15,20] Surprisingly, it appears that the electronic properties of the substituents in the *para* position, including such that are able to impose resonative effects, play little role in this high stability. In addition, the ^{1}H NMR spectra of $L^{1-4}Ti(OiPr)_2$ taken several hours following D_2O addition includes many new signals of a new species of reduced symmetry, presumed to be a polynuclear o-bridged compound with bound salan ligands as observed for related complexes (Figure 4).[26] Moreover, the integration change overtime (Figure 2) confirms that this cluster is the major hydrolysis product obtained simultaneously to isopropoxo release, based on very little formation of free salan ligand, $< 20\%$.[37] It thus seems that the hydrolytic stability of these complexes is derived mostly from the inherent nature of the phenolato moieties, and is more dramatically affected by steric groups *ortho* to the metal binding site that affect formation of a cluster by imposing a kinetic barrier,[26] rather than by electronic effects on the periphery of the aromatic rings which are negligible. Therefore, complexes that are unsubstituted at the *ortho* positions such as $L^{1-4}Ti(OiPr)_2$ all give similar hydrolysis rates.

In a previous study, we reported that $L^aTi(OiPr)_2$ (Chart 1) is remarkably stable with a half-life for isopropoxo hydrolysis of 31 h, with slow formation of a cluster because of the large *ortho* methyl substituent imposing a kinetic barrier (Figure 3).[26] We were thus interested to examine a different series of complexes, with substituents of different electronic features at the *ortho* position as well.

Hydrolysis studies conducted for $L^{5-7}Ti(OiPr)_2$ (Chart 1) indicated remarkable stability, substantially higher than that of related complexes that do not include *ortho* Cl or Br substituents,[25] despite the very small effect of the Cl substituents on the structure of $L^5Ti(OiPr)_2$ as evident by its crystal structure (Figure 1, Table 1). Monitoring the integration of the signals in the ^{1}H NMR of complexes $L^{5-7}Ti(OiPr)_2$ following D_2O addition over a period of 60 h showed extremely slow change in integration of both the bound phenolato and the presumably more labile isopropoxo ligands, (Figure 3, Table 2), and new signals of a hydrolysis product could barely be detected (Figure 4). It is thus obvious that these complexes do not undergo significant hydrolysis for days under these conditions.

$L^6Ti(OiPr)_2$ (Chart 1) featuring only *ortho*-Cl groups demonstrates similar hydrolytic stability to that of $L^5Ti(OiPr)_2$, featuring both *ortho*- and *para*-Cl substituents (Table 2, Figure 3). This supports the conclusion that electronic effects at the *para* position are of lesser significance as observed for $L^{1-4}Ti(OiPr)_2$. Adding $L^7Ti(OiPr)_2$ and $L^aTi(OiPr)_2$[26] (Chart 1) to the discussion points to this effect being mainly, but not solely, electronic, as $L^7Ti(OiPr)_2$ demonstrates even higher hydrolytic stability than that of $L^{5,6}Ti(OiPr)_2$ presumably because of the larger volume of the Br substituents, and the stability of all three $L^{5-7}Ti(OiPr)_2$ is even higher than that of $L^aTi(OiPr)_2$ featuring solely Me substituents (Table 2, Figure 3). Interestingly, the markedly enhanced hydrolytic stability is not observed for the methoxy substituted complex $L^8Ti(OiPr)_2$ with a half-life of isopropoxo hydrolysis of 3.4 h (Table 2, Figure 3) to give a cluster as the main product ($> 70\%$), despite its greater steric bulk. This supports the conclusion that this effect of hydrolytic stability enhancement in mainly electronic.

Because of the observed high water stability of $L^{5-7}Ti(OiPr)_2$, these complexes were reacted with varying equivalents of water: 50, 100, and 1000, over a 3 days period, in an attempt to structurally characterize hydrolysis products.

(37) As the polynuclear hydrolysis products are of low symmetry, the multiple signals of low integration in their ^{1}H NMR spectra make it difficult to assign complete proton identity. Therefore, the percentage of cluster formed is estimated based on the percentage of free bis(phenol) ligand released.

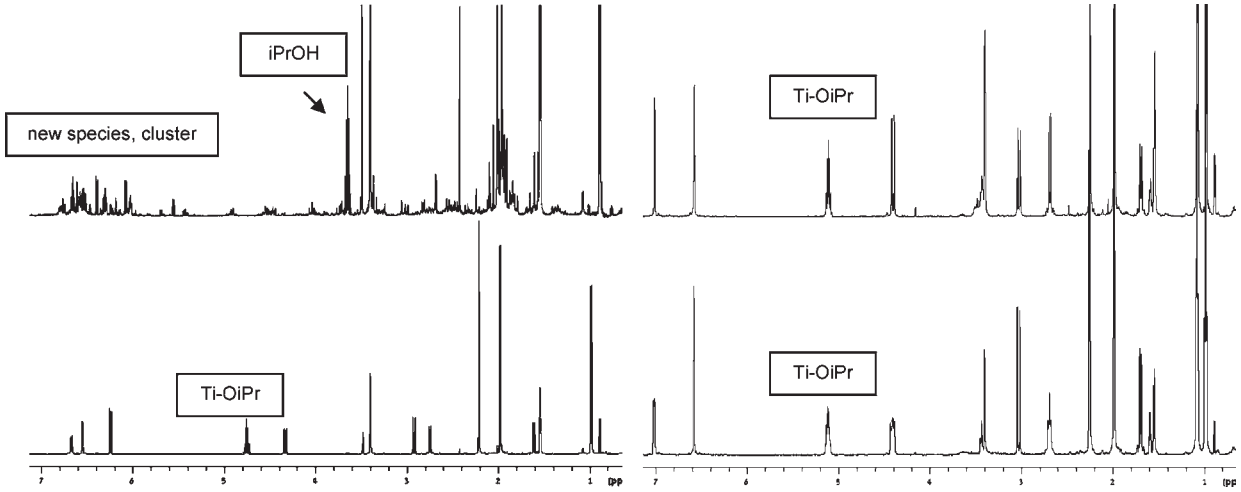

Figure 4. ^{1}H NMR spectra of $L^1Ti(OiPr)_2$ (left) and $L^7Ti(OiPr)_2$ (right) at RT in d_8-THF immediately (bottom) and 20 h (top) following addition of D_2O.

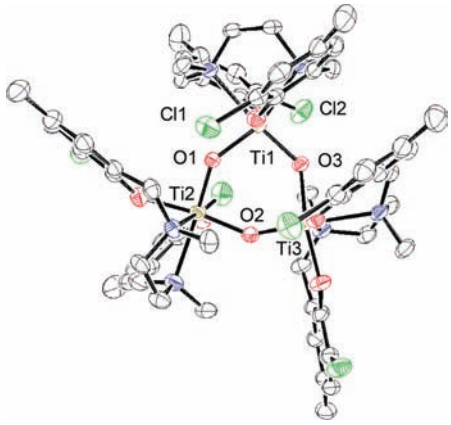

Figure 5. ORTEP drawing of $Ti_3L^6{}_3(\mu\text{-}O)_3$, the hydrolysis product of $L^6Ti(OiPr)_2$, in 50% probability ellipsoids. H atoms and disordered solvent were omitted for clarity.

Single crystals of the isolated powder obtained from the reaction of $L^5Ti(OiPr)_2$ with 100 water equivalents were analyzed by X-ray crystallography, and the structure features the starting complex $L^5Ti(OiPr)_2$ (Figure 1). This is consistent with the ^{1}H NMR spectrum of the product indicating that $L^5Ti(OiPr)_2$ is the main compound present in solution, although traces of a polynuclear product could also be detected (Supporting Information, Figure S8). This supports our conclusion regarding the high hydrolytic stability of this compound.[29] Interestingly, however, the reaction of $L^6Ti(OiPr)_2$ with 50 water equivalents yielded single crystals of the extremely minor polynuclear product as evident by ^{1}H NMR (Supporting Information, Figure S9). The crystals contain disordered diethylether and water molecules. Nevertheless, the structure of the main molecule (Figure 5, Table 3) features a trinuclear Ti(IV) complex bridged by three oxo units, with a phenolato ligand bound to each Ti(IV) center. One out of the three Ti(IV) cores (Ti(1)) retains the original *trans* configuration, while the other two (Ti(2), Ti(3)) feature *cis* binding of the phenolato units, giving altogether a symmetry of C_1. This low symmetry explains the multiple signals observed in the ^{1}H NMR for new hydrolysis products (Figure 4). The nearest Cl···Cl distance for two different ligands is 3.7 Å. This structure is generally highly similar to another cluster we previously reported formed from an *ortho*-H-*para*-Me-*meta*-Me derivative,[26] which supports the notion that similar hydrolysis pathways occur for much of the complexes of this family with different steric and electronic demands. It is thus clear that the especially stable *ortho*-halogenated compounds are also able to form the O-bridged hydrolysis products over long periods and/or under conditions of high water concentrations. A comparison of the ^{1}H NMR spectra of the hydrolysis products obtained for $L^{5-7}Ti(OiPr)_2$ reacted with 1000 water equivalents for 3 days is presented in Figure 6, which demonstrates the relative portion of polynuclear compounds obtained for these complexes and the particularly enhanced stability of $L^7Ti(OiPr)_2$. Additional ^{1}H NMR spectra of the products obtained following addition of 50 and 100 water equivalents are given in Supporting Information, Figure S7−S12.

Table 3. Selected Bond Lengths (Å) and Angles (deg) for $Ti_3L^6{}_3(\mu\text{-}O)_3$, the Hydrolysis Product of $L^6Ti(OiPr)_2$

atoms	value	atoms	value
	Lengths		
O(1)−Ti(1)	1.831(2)	N(1)−Ti(1)	2.337(3)
O(3)−Ti(1)	1.793(2)	N(2)−Ti(1)	2.368(3)
O(4)−Ti(1)	1.943(2)	N(3)−Ti(2)	2.258(3)
O(5)−Ti(1)	1.934(2)	N(4)−Ti(2)	2.361(3)
O(1)−Ti(2)	1.805(2)	N(5)−Ti(3)	2.281(3)
O(2)−Ti(2)	1.872(2)	N(6)−Ti(3)	2.354(3)
O(2)−Ti(3)	1.801(2)		
O(3)−Ti(3)	1.913(2)		
O(6)−Ti(2)	1.954(2)		
O(7)−Ti(2)	1.871(2)		
O(8)−Ti(3)	1.938(2)		
O(9)−Ti(3)	1.875(2)		
	Angles		
O(3)−Ti(1)−O(1)	101.12(9)	O(1)−Ti(2)−N(3)	93.77(9)
O(1)−Ti(2)−O(2)	92.94(9)	O(7)−Ti(2)−N(3)	155.11(10)
O(2)−Ti(3)−O(3)	95.61(9)	O(2)−Ti(2)−N(3)	89.96(9)
O(1)−Ti(2)−O(7)	109.47(10)	O(6)−Ti(2)−N(3)	79.95(9)
O(7)−Ti(2)−O(2)	97.40(10)	O(1)−Ti(2)−N(4)	170.52(10)
O(1)−Ti(2)−O(6)	91.78(9)	O(7)−Ti(2)−N(4)	79.84(10)
O(7)−Ti(2)−O(6)	90.25(10)	O(2)−Ti(2)−N(4)	87.48(10)
O(2)−Ti(2)−O(6)	169.12(10)	O(6)−Ti(2)−N(4)	86.26(10)
Ti(1)− O(1)− Ti(2)	141.47(12)	N(3)−Ti(2)−N(4)	76.76(10)
Ti(3)− O(2)− Ti(2)	146.66(12)		
Ti(1)− O(3)− Ti(3)	135.55(11)		

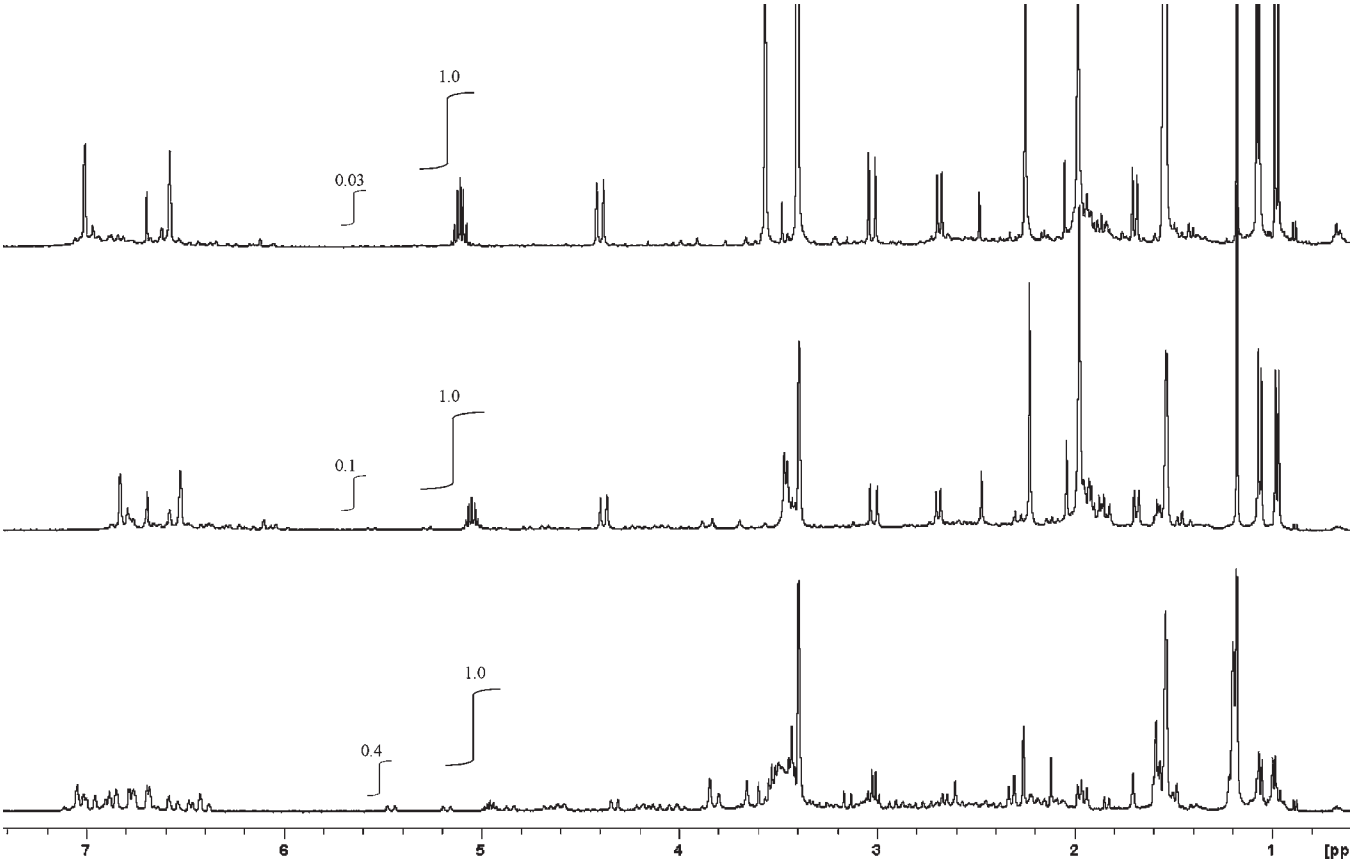

Figure 6. ^{1}H NMR spectra of $L^5Ti(OiPr)_2$ (bottom), $L^6Ti(OiPr)_2$ (middle), and $L^7Ti(OiPr)_2$ (top) 3 days following addition of 1000 water equivalents; the integration of remaining bound isopropoxo relative to a new doublet of a polynuclear hydrolysis product is presented.

Table 4. Relative IC_{50} (μM) and Maximal Cell Growth Inhibition (%) of $L^{1\text{-}8}Ti(OiPr)_2$ Towards HT-29 and OVCAR-1 Cancer Cell Lines

complex	HT-29	OVCAR-1
$L^1Ti(OiPr)_2$	6.2 ± 0.9 (90%)	5.2 ± 1.1 (79%)
$L^2Ti(OiPr)_2$	2.9 ± 0.5 (80%)	11.5 ± 2.7 (82%)
$L^3Ti(OiPr)_2$	2.6 ± 0.6 (83%)	3.3 ± 0.8 (70%)
$L^4Ti(OiPr)_2$	16.6 ± 3.8 (82%)	17.7 ± 3.6 (76%)
$L^5Ti(OiPr)_2$	2.4 ± 0.4 (51%)	2.7 ± 0.5 (52%)
$L^6Ti(OiPr)_2$	7.2 ± 2.0 (76%)	4.5 ± 0.9 (83%)
$L^7Ti(OiPr)_2$	2.0 ± 0.5 (70%)	1.5 ± 0.3 (69%)
$L^8Ti(OiPr)_2$	8.1 ± 1.6 (98%)	6.3 ± 0.9 (98%)
Cp_2TiCl_2	609 ± 4 (90%)	701 ± 4 (91%)
$(bzac)_2Ti(OiPr)_2$	15.2 ± 0.3 (92%)	14.9 ± 0.4 (91%)

We may thus conclude that the *ortho* substituents are of the largest influence on hydrolytic stability, which may impose not only steric[26] but also significant electronic effects. Consequently, as high water resistance is observed for the complexes presented herein, and yet, their ability to form clusters over long periods was established, both features proved essential for high antitumor activity in our previous studies,[26] we were eager to continue to cytotoxicity measurements.

Cytotoxicity Measurements. The cytotoxicity measurements were carried out with two types of cell lines: ovarian OVCAR-1 and colon HT-29, and analysis was achieved by the MTT (methylthiazolyldiphenyl-tetrazolium bromide) assay following 3d incubation of the cells with the complex analyzed. A summary of relative IC_{50} values and maximal cell growth inhibition are presented in Table 4, and representative plots of cell viability versus concentration toward both cell types are given in Figure 7.

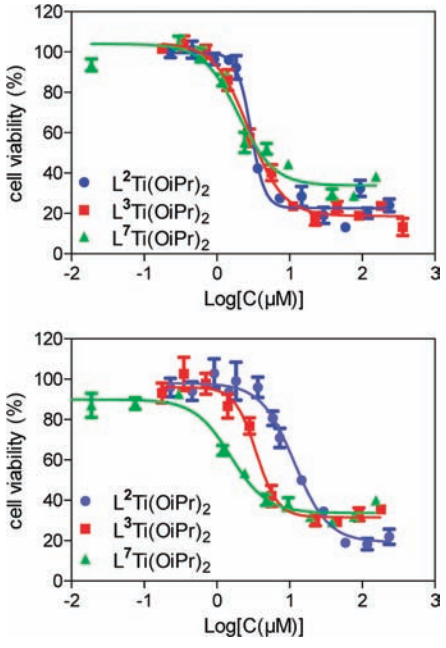

Figure 7. Dependence of HT-29 (top) and OVCAR-1 (bottom) cell viability after 3 d incubation period based on the MTT assay on administered concentration of $L^{2,3,7}Ti(OiPr)_2$ presented in logarithmic scale.

In general, we observe that the correlation between hydrolytic behavior and stability and the cytotoxic activity that we reported on previously is retained.[26] Complexes $L^{1-4}Ti(OiPr)_2$ which are substituted solely at the

para positions of the aromatic moieties (Chart 1), exhibit high cytotoxic activities with IC_{50} values between 3 and 18 μM (Table 4), activity which is also mostly higher than that of Cp_2TiCl_2, $(bzac)_2Ti(OiPr)_2$, and cisplatin toward the cells analyzed.[25] This stands in agreement with the hydrolytic behavior of $L^{1-4}Ti(OiPr)_2$, involving relatively slow hydrolysis to give polynuclear products, features that were shown in our previous studies to be essential for cytotoxic activity. In addition, as the hydrolysis is not largely influenced by the substituent electronic features, no clear dependence pattern of the cytotoxicity on the electronic donation ability of the *para* substituents can be detected, where in fact, the most active complex in this series of $L^{1-4}Ti(OiPr)_2$ is $L^3Ti(OiPr)_2$ with a IC_{50} values of 2.6 ± 0.6 and 3.3 ± 0.8 μM for the colon and ovarian cells, respectively (Table 4), which bears the most electron withdrawing groups of all, NO_2 (Chart 1). One possible reason to the highest activity of $L^3Ti(OiPr)_2$ may relate to the high planarity of the NO_2 substituents and their "flat" nature, which might support DNA intercalation taking part in the activity mechanism, and is in agreement with our previous observation regarding negative effect of large *para* substituents such as *t*-Bu on cytotoxicity.[26] On the same note, $L^{1,4}Ti(OiPr)_2$ exhibit IC_{50} values of 6.2 ± 0.9 (colon) and 5.2 ± 1.1 (ovarian), and 16.6 ± 3.8 (colon) and 17.7 ± 3.6 (ovarian) μM, respectively (Table 4). This activity difference may again be attributed to steric hindrance and interruption to planarity, rather than to different electronic effects.

The complexes halogenated at the *ortho* positions demonstrate exceptionally high cytotoxicity particularly at low concentrations with the IC_{50} values varying between 2 and 7 μM for colon cells and $1-5$ μM for ovarian cells, which may relate to their especially high hydrolytic stability.[29,38] For this series, the steric effects seem to be relatively minor, as $L^5Ti(OiPr)_2$ is more active than $L^aTi(OiPr)_2$ (Chart 1), and even higher activity is observed for $L^{6,7}Ti(OiPr)_2$ when taking maximal inhibition into consideration (Table 4). These observations may suggest that the electronic properties induced at the *ortho* position have larger effect on the cytotoxicity than the steric hindrance, perhaps because of their effect on hydrolytic stability. Furthermore, placing a substituent with higher steric hindrance such as a methoxy group at the *ortho* position ($L^8Ti(OiPr)_2$, Chart 1) produces a species with similar activity to that of $L^aTi(OiPr)_2$.

Conclusions

In this study we were interested to evaluate whether controlled substitutions with electron withdrawing and donating groups at the aromatic moieties of the tetradentate ligands at the *ortho* and at the *para* positions to the metal binding site can lead to additional insight on the hydrolytic behavior and the biological activity of this promising new family of cytotoxic Ti(IV) compounds that we recently introduced. We worked under the assumption that increasing electron donation ability of the ligands should also increase hydrolytic stability, and therefore, might affect cytotoxicity as well. We thus analyzed several complexes with varying substituents of different electronic features positioned at the *ortho* and at the *para* positions, which are largely available through a highly convenient synthetic pathway, making this family of complexes especially attractive for study and development.

High activity is observed for complexes of this family on OVCAR-1 and HT-29 cells, higher than that of Cp_2TiCl_2, $(bzac)_2Ti(OiPr)_2$, and cisplatin, which is accompanied by exceptionally high hydrolytic stability, higher than that of known Ti(IV) cytotoxic complexes. In addition, we continue to observe the relation between these parameters: highly hydrolytically stable complexes lead to high cytotoxicity. We observe that the active salan complexes very slowly give polynuclear clusters with bound phenolato ligand upon hydrolysis, involving release of the labile isopropoxo ligands as isopropanol. This is not always the case for inactive complexes, which largely release free bis(phenol) ligands because of steric hindrance or inherent hydrolytic instability.[26] We overall continue to observe a big influence of the particular ligand on the complex performance, which certainly encourages further ligand design.

We found that contrary to our assumption, varying electronic features of *para* substituents have very little influence on hydrolytic stability, identifying the diamine bis(phenolato) core as the main responsible parameter for the inherent water resistance of these complexes. The cytotoxicity, on the other hand, seems to depend much more on steric effects and the planarity of the substituents, which may be attributed to the involvement of DNA intercalation in the activity mechanism,[12] which is also in agreement with our recent report identifying the biological target as chiral.[28] Nevertheless, influence of these parameters on cell penetration cannot be ruled out.

We observed strong positive electronic influence of *ortho*-Cl and -Br substituents on hydrolytic stability, which is not observed for *para* substitution, the reason for which is not exactly clear. In particular, the *para*-methylated-*ortho*-halogenated complexes we prepared are extremely stable with no substantial release of the most labile isopropoxo ligands for days in 1:9 water/THF solutions. Moreover, these complexes demonstrate higher cytotoxicity than their analogues, with some effect of the halogen radius on hydrolysis and cytotoxicity. In addition, the eventual formation of polynuclear hydrolysis products, established based on X-ray crystallography for one compound and supported by NMR analyses of all, is in agreement with our previous studies suggesting that the steric ability to form such clusters is essential for cytotoxicity. We thus suspect one of two options: (a) the steric requirement to form the cluster is similar to that of the interaction with the biological target; (b) the original bis(isopropoxo) complex is required for cell penetration, and the cluster itself or an intermediate in its formation might be active inside the cell. Indeed, all highly cytotoxic complexes of the series studied herein form such clusters over long periods in water environment. Nevertheless, as the clusters themselves are inactive,[26] either in terms of cell penetration or of cellular interactions, it is concluded that decreasing the rate of hydrolysis to give them is of importance for enhancing cytotoxic activity of diamino bis(phenolato) "salan" Ti(IV) complexes. Therefore, the *para*-Me-*ortho*-Br complex $L^7Ti(OiPr)_2$ exhibits the highest cytotoxic activity of all, accompanied by incredibly high water stability, and represents the most promising antitumor Ti(IV) complex of this family identified thus far.

In conclusion, electronic variation enabled as to isolate readily available salan Ti(IV) complexes of especially high

(38) Immel, T. A.; Debiak, M.; Groth, U.; Burkle, A.; Huhn, T. *ChemMedChem* **2009**, *4*, 738–741.

hydrolytic stability and cytotoxicity. Additional mechanistic studies relating to the hydrolysis pathway and its relation to the cytotoxicity mechanism are underway.

Experimental Section

Ligands and their bis(isopropoxo) Ti(IV) complexes were synthesized according to published procedures.[30−34] Data on H_2L^{1-4},[31] H_2L^5,[34] H_2L^8,[39] $L^3Ti(OiPr)_2$,[33] $L^5Ti(OPr)_2$,[34] and $L^8Ti(OiPr)_2$[39] can be found elsewhere. Paraformaldehyde, *N*, *N*′-dimethylethylenediamine and all substituted phenol compounds were purchased from Aldrich Chemical Co. Inc. or Fluka Riedel-deHaën. Titanium tetra(isopropoxide) (97%) was purchased from Aldrich Chemical Co., Inc. All solvents were distilled from K or K/benzophenone under nitrogen. All experiments requiring dry atmosphere were performed in a M. Braun drybox or under nitrogen atmosphere using Schlenk line techniques. NMR data were recorded using AMX-400 MHz or AMX-500 MHz Bruker spectrometer. X-ray diffraction data were obtained with a Bruker SMART APEX CCD diffractometer, running the SMART software package. After collection, the raw data frames were integrated by the SAINT software package. The structures were solved and refined using the SHELXTL software package. Elemental analyses were performed in the microanalytical laboratory in our institute. Kinetic studies by NMR to monitor hydrolysis of isopropoxo groups to give polynuclear products, for the establishment of relative water resistance, were performed using about 6 mM of the complex solution in d_8-THF and adding D_2O to give a final solution of 1:9 D_2O/d_8-THF, with added D_2O being > 1000 equivalents relative to Ti(IV). The average $t_{1/2}$ value based on a pseudo first order fit (Supporting Information, Figure S2) of three replicates is reported for each compound. The results were verified by including *p*-dinitro benzene as an internal standard. The sum of integration of iPrOH and Ti-OiPr in the first measurement following D_2O addition was assigned as integration 1. Attempts to crystallize the hydrolysis products were performed using 2−20 mM of the complex as a THF solution and adding 50, 100, or 1000 water equivalents.

Cytotoxicity was measured on HT-29 colon and OVCAR-1 ovarian cells obtained from ATCC Inc. using the methylthiazolyldiphenyl-tetrazolium bromide (MTT) assay. In more detail: cells (1.2×10^6) in medium (contains: 1% penicillin/streptomycin antibiotics; 1% L-glutamine; 10% fetal bovine serum (FBS), all purchased from Biological Industries Inc., and 88% medium RPMI-1640, purchased from Sigma Inc.) were seeded into a 96-well plate and allowed to attach for 24 h. The cells were consequently treated with the reagent tested at 10 different concentrations. Solution of reagent was prepared by dissolving the reagent in 10 μL of the suitable solvent (THF or H_2O) and diluting with 90 μL of medium to give final concentrations of up to 200 mg/L. From the resulting solution, 10 μL was added to each well already containing 200 μL of the above solution of cells in the medium. After a standard of 3 days incubation at 37 °C in 5% CO_2 atmosphere, MTT (0.1 mg in 20 μL) was added, and the cells were incubated for additional 3−4 h. The MTT solution was then removed, and the cells were dissolved in 200 μL of isopropanol. The absorbance at 550 nm was measured for 100 μL of the above solution by a Bio-Tek EL-800 microplate reader spectrophotometer. Each measurement was repeated at least 2 × 5 times, namely, two repeats per plate, all repeated five times on different days (10 repeats altogether). Relative IC_{50} values were determined by a nonlinear regression of a variable slope (four parameters) model. Control experiments were also conducted with free ligands and solvent alone. In some cases, a decrease in activity is observed at high concentration, which may be due to enhanced aggregation to give inactive polynuclear products.

L^6H_2. A solution of 2-chloro-4-methylphenol (0.59 mL, 5.0 mmol), *N*,*N*′-dimethylethylenediamine (0.27 mL, 2.5 mmol) and paraformaldehyde (0.30 g, 12 mmol) in methanol (5 mL) was stirred and refluxed for 24 h. The mixture was cooled and the colorless precipitate was filtered and washed with cooled methanol (0.85 g, 86%). ^{1}H NMR ($CDCl_3$) δ 7.07 (2H, d, J = 2.1 Hz, Ar), 6.66 (2H, d, J = 1.9 Hz, Ar), 3.67 (4H, s, CH_2), 2.69 (4H, s, CH_2), 2.30 (6H, s, CH_3), 2.21 (6H, s, CH_3); ^{13}C NMR ($CDCl_3$) δ: 151.1, 129.6, 129.1, 127.6, 122.3, 120.4, 61.6, 54.3, 41.9, 20.3; Anal. Calcd for $C_{20}H_{26}Cl_2N_2O_2$: C, 60.46; H, 6.60; N, 7.05. Found: C, 60.49; H, 6.74; N, 7.04.

L^7H_2. was synthesized similarly from 2-bromo-4-methylphenol (0.24 mL, 2.0 mmol), *N*,*N*′-dimethylethylenediamine (0.11 mL, 1.0 mmol), and paraformaldehyde (0.09 g, 3.0 mmol) (0.31 g, 63%). ^{1}H NMR ($CDCl_3$) δ 7.24 (2H, m, Ar), 6.71 (2H, m, Ar), 3.66 (4H, s, CH_2), 2.70 (4H, s, CH_2), 2.30 (6H, s, CH_3), 2.22 (6H, s, CH_3); ^{13}C NMR ($CDCl_3$) δ 152.0, 132.5, 129.6, 128.3, 122.2, 109.8, 61.6, 54.3, 41.8, 20.2; Anal. Calcd for $C_{20}H_{26}Br_2N_2O_2$: C, 49.40; H, 5.39; N, 5.76. Found: C, 49.64; H, 5.46; N, 5.52.

$L^1Ti(OiPr)_2$. $Ti(OiPr)_4$ (0.050 g, 0.18 mmol) was dissolved in 5 mL of dry THF under inert atmosphere. L^1H_2 (0.065 g, 0.18 mmol) was dissolved in 10 mL of dry THF under inert atmosphere. The two solutions were combined and allowed to mix under ambient conditions at room temperature for 2 h. The solvent was removed with reduced pressure to give the product in a quantitative yield, which may then be recrystallized from diethylether (0.028 g, 32%). ^{1}H NMR ($CDCl_3$) δ 6.96 (2H, dd, J = 8.1, 2.2 Hz, Ar), 6.74 (2H, d, J = 1.9 Hz, Ar), 6.57 (2H, d, J = 8.1 Hz, Ar), 5.02 (2H, sept, J = 6.1 Hz, OC*H*(CH_3)$_2$), 4.62 (2H, d, J = 13.4 Hz, CH_2), 3.06 (2H, d, J = 13.5 Hz, CH_2), 2.99 (2H, d, J = 9.3 Hz, CH_2), 2.44 (6H, s, CH_3), 2.24 (6H, s, CH_3), 1.76 (2H, d, J = 9.4 Hz, CH_2), 1.24 (12H, d, J = 6.1 Hz, OCH(C*H*$_3$)$_2$); ^{13}C NMR ($CDCl_3$) δ 159.8, 129.9, 129.5, 126.4, 124.3, 117.2, 77.6, 64.5, 51.8, 47.2, 26.0, 25.7, 20.5; Anal. Calcd for $C_{26}H_{40}N_2O_4Ti$: C, 63.41; H, 8.19; N, 5.69. Found: C, 63.41; H, 8.05; N, 5.49.

$L^2Ti(OiPr)_2$. was synthesized similarly in quantitative yield from $Ti(OiPr)_4$ (0.050 g, 0.18 mmol) and L^2H_2 (0.069 g, 0.18 mmol), and may be recrystallyzed from diethylether (0.039 g, 41%). ^{1}H NMR ($CDCl_3$) δ 7.10 (2H, dd, J = 8.6, 2.6 Hz, Ar), 6.92 (2H, d, J = 2.6 Hz, Ar), 6.59 (2H, d, J = 8.6 Hz, Ar), 4.96 (2H, sept, J = 6.2 Hz, OC*H*(CH_3)$_2$), 4.57 (2H, d, J = 13.8 Hz, CH_2), 3.09 (2H, d, J = 13.6 Hz, CH_2), 2.96 (2H, d, J = 9.4 Hz, CH_2), 2.43 (6H, s, CH_3), 1.84 (2H, d, J = 9.4 Hz, CH_2), 1.23 (6H, d, J = 6.1 Hz, OCH(C*H*$_3$)$_2$), 1.22 (6H, d, J = 6.1 Hz, OCH(C*H*$_3$)$_2$); ^{13}C NMR ($CDCl_3$) δ 160.7, 129.0, 125.9, 121.7, 118.8, 78.4, 77.2, 63.9, 51.8, 47.2, 25.9, 25.6; Anal. Calcd for $C_{24}H_{34}Cl_2N_2O_4Ti$: C, 54.05; H, 6.43; N, 5.25. Found: C, 54.07; H, 6.57; N, 5.08.

$L^4Ti(OiPr)_2$. was synthesized similarly in quantitative yield from $Ti(OiPr)_4$ (0.050 g, 0.18 mmol) and L^4H_2 (0.063 g, 0.18 mmol), and may be recrystallyzed from diethylether (0.041 g, 43%). ^{1}H NMR ($CDCl_3$) δ 6.73 (2H, dd, J = 8.6, 3.4 Hz, Ar), 6.60 (2H, d, J = 8.8 Hz, Ar), 6.53 (2H, d, J = 3.2 Hz, Ar), 5.03 (2H, sept, J = 6.1 Hz, OC*H*(CH_3)$_2$), 4.63 (2H, d, J = 14.0 Hz, CH_2), 3.74 (6H, s, OCH_3), 3.06 (2H, d, J = 14.0 Hz, CH_2), 2.99 (2H, d, J = 9.4 Hz, CH_2), 2.44 (6H, s, CH_3), 1.78 (2H, d, J = 9.4 Hz, CH_2), 1.24 (6H, d, J = 6.1 Hz, OCH(CH_3)$_2$, 1.23 (6H, d, J = 6.1 Hz, OCH(C*H*$_3$)$_2$); ^{13}C NMR ($CDCl_3$) δ 156.2, 151.3, 125.0, 117.7, 115.0, 113.9, 77.6, 64.5, 55.8, 51.9, 47.1, 26.0, 25.7; Anal. Calcd for $C_{26}H_{40}N_2O_6Ti$: C, 59.54; H, 7.69; N, 5.34. Found: C, 59.03; H, 7.19; N, 5.32.

Crystal Data for $L^5Ti(OiPr)_2$. $C_{24}H_{32}Cl_4N_2O_4Ti$, M = 602.22, monoclinic, a = 8.8097(5), b = 12.7717(8), c = 25.197(2) Å, β = 97.547(1)°, V = 2810.5(3) Å^3, T = 223(1) K, space group $P2_1/c$, Z = 4, μ(Mo−Kα) = 0.717 mm^{-1}, 30700 reflections measured, 6144 unique (R_{int} = 0.0281). Observed reflections [$I > 2\sigma(I)$] = 5809 for which R = 0.0815 and wR_2 = 0.1734.

(39) Kim, S. H.; Lee, J.; Kim, D. J.; Moon, J. H.; Yoon, S.; Oh, H. J.; Do, Y.; Ko, Y. S.; Yim, J. H.; Kim, Y. *J. Organomet. Chem.* **2009**, *694*, 3409–3417.

$L^6Ti(OiPr)_2$. was synthesized similarly in quantitative yield from $Ti(OiPr)_4$ (0.050 g, 0.18 mmol) and L^6H_2 (0.070 g, 0.18 mmol), and may be recrystallyzed from diethylether (0.041 g, 41%). ^1H NMR ($CDCl_3$) δ 7.09 (2H, d, J = 1.9 Hz, Ar), 6.66 (2H, d, J = 1.6 Hz, Ar), 5.32 (2H, sept, J = 6.1 Hz, $OCH(CH_3)_2$), 4.68 (2H, d, J = 13.5 Hz, CH_2), 3.10 (2H, d, J = 13.5 Hz, CH_2), 2.95 (2H, d, J = 9.6 Hz, CH2), 2.45 (6H, s, CH_3), 2.21 (6H, s, CH_3), 1.79 (2H, d, J = 9.4 Hz, CH_2), 1.32 (6H, d, J = 6.0 Hz, $OCH(CH_3)_2$, 1.22 (6H, d, J = 6.2 Hz, $OCH(CH_3)_2$); ^{13}C NMR ($CDCl_3$) δ 155.1, 129.8, 128.5, 126.8, 125.4, 121.3, 78.4, 64.4, 51.6, 47.0, 26.1, 25.6, 20.3; Anal. Calcd for $C_{26}H_{38}Cl_2N_2O_4Ti$: C, 55.63; H, 6.82; N, 4.99. Found: C, 55.47; H, 6.92; N, 4.79.

$L^7Ti(OiPr)_2$. was synthesized similarly in quantitative yield from $Ti(OiPr)_4$ (0.050 g, 0.18 mmol) and L^7H_2 (0.086 g, 0.18 mmol), and may be recrystallyzed from diethylether (0.054 g, 46%). ^1H NMR ($CDCl_3$) δ 7.27 (2H, d, J = 1.5 Hz, Ar), 6.70 (2H, d, J = 1.4 Hz, Ar), 5.36 (2H, sept, J = 6.1 Hz, $OCH(CH_3)_2$), 4.69 (2H, d, J = 13.5 Hz, CH_2), 3.09 (2H, d, J = 13.6 Hz, CH_2), 2.49 (2H, d, J = 9.4 Hz, CH_2), 2.46 (6H, s, CH_3), 2.21 (6H, s, CH_3), 1.79 (2H, d, J = 9.4 Hz, CH_2), 1.31 (6H, d, J = 6.1 Hz, $OCH(CH_3)_2$), 1.22 (6H, d, J = 6.2 Hz, $OCH(CH_3)_2$); ^{13}C NMR ($CDCl_3$) δ 156.1, 132.8, 129.4, 127.3, 125.1, 111.8, 78.5, 64.5, 51.6, 47.3, 26.1, 25.7, 20.1; Anal. Calcd for $C_{26}H_{38}Br_2N_2O_4Ti$: C, 48.02; H, 5.89; N, 4.31. Found: C, 48.08; H, 5.59; N, 4.09.

Crystal Data for $Ti_3L^6_3(\mu\text{-}O)_3$. $C_{60}H_{72}Cl_6N_6O_9Ti_3 \cdot (C_4H_6O)_2(H_2O)_{0.5}$, M = 1532.36, triclinic, a = 12.9257(7), b = 14.3936(8), c = 22.576(1) Å, α = 101.578(1), β = 97.023(1), γ = 110.178(1)°, V = 3777.4(4) Å^3, T = 173(1) K, space group $P\bar{1}$, Z = 2, μ(Mo−Kα) = 0.581 mm^{-1}, 42004 reflections measured, 16287 unique (R_{int} = 0.0225). Observed reflections [$I > 2\sigma(I)$] = 13890 for which R = 0.0646 and wR_2 = 0.1886. Refinement of the structure revealed along with the well behaved complex, also three ill resolved and heavily disordered diethylether fragments. These fragments were treated with restraints (O−C:1.40 and C−C:1.50\%A) using the DFIX option of SHELXL-97 and refined isotropically.

Acknowledgment. We thank Dr. Shmuel Cohen for crystallography. This research received funding from the European Research Council under the European Community's Seventh Framework Programme (FP7/2007-2013)/ERC Grant agreement n° [239603]. The research was also partly supported the Israel Science Foundation (Grant 124/09) and the Israel Cancer Research Fund (ICRF).

Supporting Information Available: Crystallographic data for $L^5Ti(OiPr)_2$ and $Ti_3L^6_3(\mu\text{-}O)_3$, a representative ^1H NMR spectrum taken through a hydrolysis study of $L^1Ti(OiPr)_2$ with proton assignment, 1st order fits of Ti-OiPr hydrolysis for $L^{1-8}Ti(OiPr)_2$, hydrolysis studies of $L^{2-4,8}Ti(OiPr)_2$, ^1H NMR spectra following water addition of $L^{5-7}Ti(OiPr)_2$, and cytotoxicity plots of $L^{1,4,5,6,8}Ti(OiPr)_2$ toward HT-29 and OVCAR-1 cells. This material is available free of charge via the Internet at http://pubs.acs.org.